For. Sci. XX(XX):1–13
doi: 10.1093/forsci/fxz061

biometrics

A Growth and Yield Model for *Eucalyptus benthamii* in the Southeastern United States

Kevin B. Hall, J.L. Stape, Bronson P. Bullock, Doug Frederick, Jeff Wright, Henrique F. Scolforo, and Rachel Cook

In recent *Eucalyptus* cold-tolerance trials, *E. benthamii* has shown good growth rates as well as cold tolerance for USDA Plant Hardiness Zones 8 and 9. This study developed growth and yield models for *E. benthamii* in the southeastern United States. A network of 182 temporary sample plots of *E. benthamii* ranging in age from 1.5 to 13.3 years was established, and inventory data were collected. Site quality was determined by fitting a polymorphic site index curve, whereas a function for stand basal area based on age, dominant height, and site occupancy was fitted. Stand-level volume and dry-weight biomass prediction equations were fitted as a function of dominant height and basal area. Based on the growth and yield model results, mean annual increments ranged from 26.4 m^3 ha^{-1} $year^{-1}$ at rotation age 6 years on the best sites to 13.7 m^3 ha^{-1} $year^{-1}$ at rotation age 10 years on the poorest sites. This is the first published set of management-oriented models for land managers considering planting *E. benthamii* in the southeastern United States.

Keywords: short-rotation woody crops, cold-tolerant *Eucalyptus*, biomass, site index, basal area

The southeastern United States (SE US) is often referred to as the wood basket of the United States because of pine plantation success and producing more industrial timber than any other region in the world (Schultz 1997, Allen et al. 2005). The SE US will be required to use a variety of species including perennial crops and management practices as a potential fuel source to help meet the anticipated future biomass market demand (Perlack et al. 2005). This need will require the matching of species and management practices to a variety of edaphic and climatic conditions (Simmons et al. 2008). At present, successful examples of the matching of species, management, and physiographic region include *Populus* clones that outperform willow clones under coppice management in Michigan by approximately 30 percent (Wang and MacFarlane 2012). Hybrid poplar clones have been successfully planted in the north central United States on marginal agricultural fields (Goerndt and Mize 2008, Headlee et al. 2013). Netzer et al. (2002) reported that the yield of hybrid poplar total aboveground biomass (25-tree blocks) on better sites (former agricultural fields) in Wisconsin, Minnesota, and the eastern region of the Dakotas averaged 9 Mg ha^{-1} $year^{-1}$ on sites with current mean annual increment (MAI) maximized between years 7 and 11. Although there are several examples of matching species and environments for *Populus* species and willow, there are few examples of innovative forest management regimes for the SE US.

Eucalyptus has been investigated as another species with potential future for a biomass market in the SE US. This species has desirable wood properties including short fibers and high wood densities best for the production of pulp and paper, charcoal, fuel, and sawn timber (Rockwood et al. 2008). *Eucalyptus* species have been grown commercially in central and southern Florida primarily for the production of mulchwood since the 1970s (Rockwood 2012). However, the cold tolerance of certain *Eucalyptus* species, such as *E. grandis*, has limited the northern expansion of these plantation forests beyond central Florida.

The demand for short-rotation hardwood plantations for pulp and paper as well as the potential future of a biomass market increased interest in testing the adaptability and performance of cold-tolerant *Eucalyptus* species in the SE US. This demand, as well as recent success in other countries, generated interest in screening a variety of *Eucalyptus* species for cold tolerance and productivity in the SE US during the late 2000s and early 2010s. Although cold-tolerant *Eucalyptus* species have been investigated in the SE US for more than 40 years, only recently has *Eucalyptus benthamii* (*E. benthamii*) shown tolerance to drought, frost, and low temperatures (Kellison et al. 2013, Hall 2015). Indeed, this species has survived in absolute minimum temperatures ranging from –6 to –10° C, as previously observed in China (Mujiu et al. 2003).

Manuscript received August 8, 2018; accepted August 22, 2019; published online November 5, 2019.

Affiliations: *Kevin B. Hall (kbhall2@icloud.com), J. L. Stape (stape@suzano.com.br) and Henrique F. Scolforo (hscolforo@suzano.com.br), Suzano Pulp and Paper, Itapetininga, SP, Brazil. Bronson P. Bullock (bronsonbullock@uga.edu), University of Georgia, Athens, GA. Doug Frederick (dfred@ncsu.edu) and Rachel Cook (rlcook@ncsu.edu), North Carolina State University, Raleigh, NC. Jeff Wright (patula.wright@gmail.com), Durania LLC, Boone, NC.*
Acknowledgments: *This work was supported by the Forest Productivity Cooperative and its members and the Southern Partnership for Integrated Biomass Supply Systems (grant no. 2011-68005-30410/project accession no. 0225502) from the USDA National Institute of Food and Agriculture.*

Eucalyptus benthamii was first introduced in the SE US during the 1990s by Westvaco Corporation and has shown good tolerance to freezing temperatures (Zalesny et al. 2011). Although current literature has estimated potential productivity of cold-tolerant *Eucalyptus* in the SE US (Stanturf et al. 2018), continued research is necessary to quantify the actual productivity of *E. benthamii* in the SE US to evaluate the yield gap and provide empirical evidence to aid in economic decisions related to forest management.

The purpose of this research was to model the current yield of cold-tolerant *E. benthamii* in the SE US. The objectives of this study were (1) to develop site index (SI) curves, (2) to develop a growth and yield (G & Y) model to estimate the stand-level volume and dry weight biomass for *E. benthamii*, and (3) to evaluate current (CAI) and MAI curves for projected rotation ages. This study is intended to produce initial simple and easy-to-use G & Y models for a novel species in the SE US. Studies using these approaches to highlight *Eucalyptus* productivity and potential have been previously conducted in Brazil by Scolforo et al. (2016) and Scolforo et al. (2017); however, no such work has been done in the United States. This study provides the first assessment of SI, basal area, and yield functions to show the productivity of *E. benthamii* in the SE US.

Materials and Methods

Characterization of Study Area and Database

The Forest Productivity Cooperative (FPC) cold-tolerance *Eucalyptus* species screening trial (termed the Regionwide 24 or RW24) was established with 150 species across the SE US. After three years, seven species showed sufficient cold-hardiness through the 2010, 2011, and 2012 winters, with *E. benthamii* being the best performer in growth, canopy health, and survival (Hall 2015). Additional sample plots were subsequently installed outside the RW24 screening trial across the SE US in various stand sizes ranging from small study plots to operational forest plantations to be used in conjunction with the FPC cold tolerance biomass trials to assess the actual productivity of *E. benthamii* (Table 1).

E. benthamii temporary sample plots were established across the SE US to encompass many growing conditions and to provide a realistic view of actual production. One hundred and eighty-two sample plots (stand ages ranged from 1.5 to 13.3 years in age in 2012 and 2013) were installed in the 25 sites to examine the productivity of *E. benthamii* (Figure 1). One hundred and sixty-two *E. benthamii* rectangular plots were included from the FPC RW24 biomass trials, and an additional 20 circular plots were installed outside the FPC network. Additional plots were included outside the FPC network to capture more diverse growing conditions, where plot centers were established between two dominant or codominant trees, and all trees were tagged (Figure 2). Plot sizes ranged from 113 to 314 m^2.

Sites ranged in longitude from 77.38°W (eastern North Carolina) to 94.48°W (eastern Texas) and in latitude from 29.48°N (southern Florida) to 35.82°N (central North Carolina). Sites were predominantly established on sandy soils with elevations ranging from 7 to 132 m above sea level, and 30-year annual minimum temperatures ranging from 9.7° C to 15.9° C (Soil Survey Staff; Arguez et al. 2012) (Table 2).

Diameter at 1.37 m above ground (*dbh*) was measured for all trees, and total height (*h*) was measured for the first six trees (as numbered in Figure 2) in the sample plot. Additionally, dominant height (*H*) was measured based on the mean top height concept, which is equivalent to the average height of the 100 largest trees in dbh per hectare. A minimum of two dominant trees were selected per plot, and at least 10 tree heights were measured per plot. On average, 40 percent of the tree heights were measured within the permanent inventory plots. Hence, all heights of dominant and codominant trees based on the mean top height concept were measured. Heights were estimated for the remaining trees within each plot using the height–diameter equation form ($\ln h = \beta_0 + \beta_1 dbh^{-1}$) presented by Curtis (1967) where parameter estimates were estimated for each sample plot. The following individual tree stem volume (termed *v*) and dry weight biomass (termed *dw*) equations derived from destructively sampled *E. benthamii* in the SE US (unpublished data) were used to estimate the total stem yield for each inventory plot:

$$\ln \hat{v} = -9.698 + 1.780 \ln dbh + 1.020 \ln h \qquad (1)$$

$$\ln \widehat{dw} = -3.550 + 1.710 \ln dbh + 1.180 \ln h \qquad (2)$$

where all terms were previously defined.

G & Y Model—System of Equations

Statistical analyses were performed using the package stats in the software R (R Core Team 2015). Residuals graphs, parameter significance and its standard error, coefficient of determination (R^2), root mean square error (RMSE), Bayesian information criteria (BIC), and mean bias error (MBE) were used to assess the goodness of fit for each model. These figures and terms were used to assess model assumptions related to independence, normality, and variance.

Dominant Height Equation

A range of stand characteristics such as climate, intensive management regimes, and genetic stock can influence SI, to reflect the changes in site quality (Burkhart and Tomé 2012). This study examined the performance of four SI model forms for *E. benthamii* to assess site quality. The logarithm of height–reciprocal of age model presented by Schumacher (1939) (Equation 3), the Chapman–Richards (Equation 4), the Logistic (Equation 5), and the Bailey–Clutter (Equation 6) growth functions were fitted to predict dominant height:

Management and Policy Implications

Short-rotation woody crops can help meet future feedstock demands. *Eucalyptus* species have been introduced around the world to meet global fiber and energy demands. Cold-tolerant *Eucalyptus* species are used with great success in the Southern Hemisphere outside traditional tropical and subtropical climates. Many of these species have been tested in the southeastern United States, and *Eucalyptus benthamii* have shown significant cold tolerance and promising growth. However, management of *Eucalyptus* is considerably different to the management of native pine and hardwood plantations, and there is a critical need for a growth and yield model for *E. benthamii* in the southeastern United States. Growth and yield models provide landowners, managers, and investors an empirical framework to make decisions related to management regimes and production predictions based on actual stand conditions.

Table 1. Identification and description of the seedlots tested in the regionwide 24 cold-tolerant *Eucalyptus* screening trials included and presented in this growth and yield analysis.

Identification	Source	Country	Seedlot	Study site	Latitude	Longitude
BEN1390	CSIRO	Australia	21171	246302	31.306	–83.798
BEN1393	CSIRO	Australia	20880	246302	31.306	–83.798
BEN1402	IPEF—Golden Tree	Brazil	Unknown	244202	31.417	–82.325
				246302	31.306	–83.798
BEN155	IPEF—Valor Florestal	Brazil	Unknown	244202	31.417	–82.325
				245805	29.478	–81.994
				246302	31.306	–83.798
BEN5	IPEF—Golden Tree	Brazil	Unknown	241103	30.692	–93.486
				241302	34.845	–77.379
				246201	31.686	–87.963
				246301	31.305	–83.798
BEN6	IPEF—Valor Florestal	Brazil	Unknown	240701	32.997	–81.378
				241103	30.692	–93.486
				244201	31.418	–82.326
				246201	31.686	–87.963
				246301	31.305	–83.798
BEN7	SAPPI	South Africa	EB66716	241103	30.692	–93.486
				246201	31.686	–87.963
BEN77	CSIRO	Australia	Unknown	246201	31.686	–87.963
BEN78	CSIRO	Australia	unknown	240701	32.997	–81.378
				246101	26.859	–81.399
				246201	31.686	–87.963

Note: Several seedlots were tested at various locations (Study site) across the southeastern United States. Seedlot source identification number is included when available.

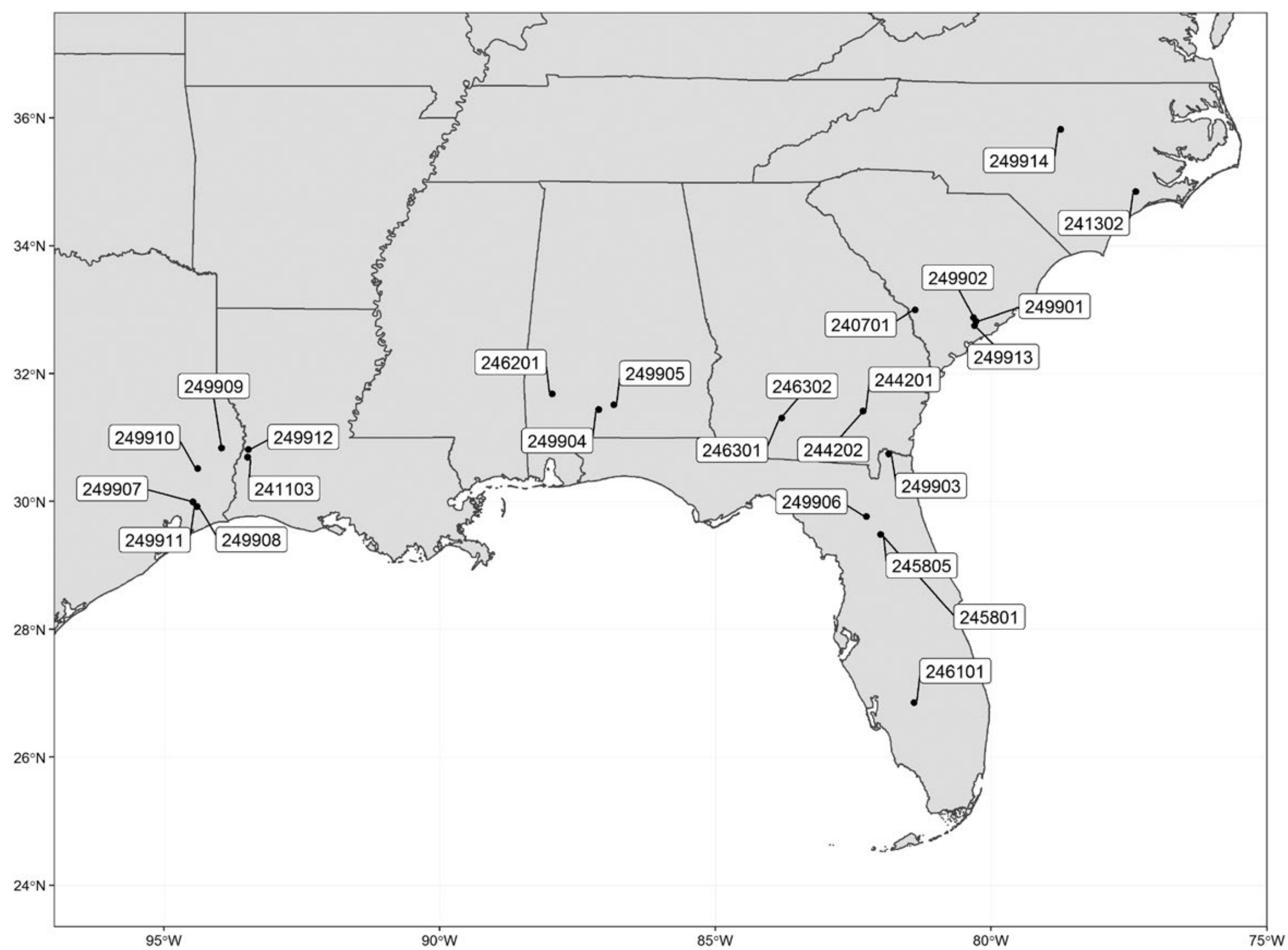

Figure 1. ***E. benthamii*** **inventory plot network across the SE US.**

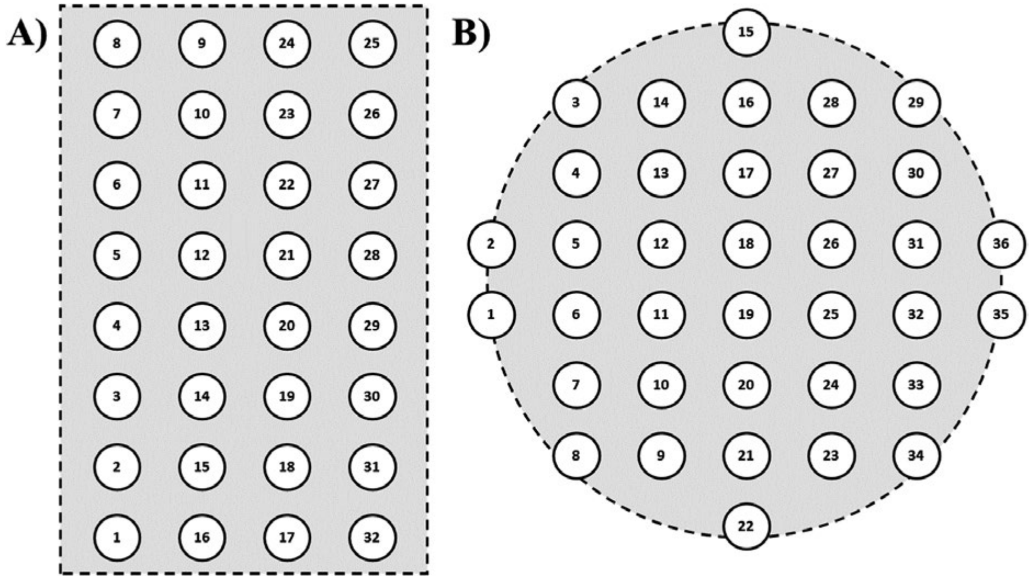

Figure 2. Schematic representation of rectangular (A) and circular (B) permanent sample plots (dotted line with gray fill) and measurement sequence (number) of sample trees (solid line with white fill).

$$\ln H = \beta_0 + \beta_1 A^{-1} + \varepsilon \quad (3)$$

$$H = \beta_2 \left(1 - e^{(\beta_3 A)}\right)^{\beta_4} + \varepsilon \quad (4)$$

$$H = \frac{\beta_5}{\left[1 + \beta_6 e^{(\beta_7 A)}\right]} + \varepsilon \quad (5)$$

$$H = \beta_8 e^{\left(\beta_9 A^{-\beta_{10}}\right)} + \varepsilon \quad (6)$$

where H is dominant height (m), β_i ($i = 0, \ldots, 10$) are parameters to be estimated, and A is age (years) of the tree since planting

Basal Area Equation

Basal area is one metric used by forest managers to assess stand density and is highly correlated with stand-level volume (Burkhart and Tomé 2012). Basal area is a key component of stand G & Y models, i.e., it is highly correlated with stand G & Y with the inclusion of stand age and SI (Burkhart and Tomé 2012). Pienaar and Shiver (1986) explain that long-term spacing studies have shown that basal area increases asymptotically with age, and the asymptote is dependent on site quality and stand density. Hence, the following equations were fitted to predict stand-level basal area:

$$\ln B = \beta_{11} + \beta_{12} A^{-1} + \beta_{13} \left(\frac{S}{A}\right) + \varepsilon \quad (7)$$

$$\ln B = \beta_{14} + \beta_{15} A^{-1} + \beta_{16} \ln H + \beta_{17} N + \varepsilon \quad (8)$$

$$\ln B = \beta_{18} + \beta_{19} A^{-1} + \beta_{20} \ln H + \beta_{21} RS + \varepsilon \quad (9)$$

where B is the basal area (m^2 ha^{-1}), S is SI at base age 7 years, N is trees per hectare, RS is the relative spacing and defined as $\frac{\sqrt{\frac{10000}{N}}}{H}$ (Zhao et al. 2012), β_i ($i = 11, \ldots, 21$) are the parameters to be estimated, and all other terms were previously defined.

Stand-Level Yield Equations

Yield at any age is typically described as a function of some measure of site quality and stocking (Burkhart and Tomé 2012). Hence, using a constant form factor (F), a model for stand-level volume, for instance, can be derived:

$$V = (F)(H)(B) \quad (10)$$

where V is stand-level volume (m^3 ha^{-1}), H is dominant height (m), and B is basal area (m^2 ha^{-1}).

This approach was adopted to estimate two yield types (Y) for *E. benthamii* in the SE US: stand-level volume (V; m^3 ha^{-1}) and dry weight biomass (DW; Mg ha^{-1}), which resulted in the following linear equation form:

$$\ln Y = \beta_{22} + \beta_{23} B + \beta_{24} H + \varepsilon \quad (11)$$

where β_i ($i = 22, \ldots, 24$) are the parameters to be estimated, and other terms were previously defined.

Assessing the Uncertainty Effect on the System of Equations (G & Y model)

We acknowledge that the G & Y model developed here has the inconvenience of propagation of error through the system of prediction equations, since they are all independently fitted (McRoberts and Westfall 2014). In addition, the data concentration at younger ages also has the inconvenience of increasing the uncertainty of the overall dominant height, basal area, volume, and DW biomass predictions.

The propagation of error in a system of equations can be problematic for forest management decisionmaking. The original dataset (n = 182) was sampled through nonparametric bootstrapping with replacement generating five unique datasets of each size (n = 182) to fit the dominant height (Equation 6) to each of the generated datasets. Each of the five datasets created from the bootstrapping exercise of dominant height was then sampled through nonparametric bootstrapping with replacement to yield 25 unique datasets to fit basal area (Equation 9). Each of the 25 unique datasets generated to address uncertainty related to the basal area model

Table 2. Identification and description of the sites in the Regionwide 24 cold-tolerant *Eucalyptus* screening trials included and presented in this growth and yield analysis.

Study Site	State	County	Latitude	Longitude	Elevation	Soil description	Weather station	Maximum temperature (°C)	Average temperature (°C)	Minimum temperature (°C)	Precipitation (mm)
249914	NC	Wake	35.821	−78.739	132	Cecil sandy loam	Raleigh State Univ	22.0	15.8	9.7	1,169
241302	NC	Onslow	34.845	−77.379	15	Pantego mucky loam	Jacksonville EOC	23.3	16.8	10.2	1,379
240701	SC	Allendale	32.997	−81.378	68	Uchee sand	Allendale 2 NW	24.9	17.7	10.6	1,177
249902	SC	Dorchester	32.880	−80.322	7	Mouzon fine sandy loam	Walterboro 1 SW	24.4	17.8	11.2	1,200
249913	SC	Charleston	32.754	−80.303	15	Chipley loamy fine sand	Edisto Island Middleton	24.4	19.2	13.9	1,267
249901	SC	Charleston	32.817	−80.275	11	Wagman loamy fine sand	Edisto Island Middleton	24.4	19.2	13.9	1,267
244201	GA	Pierce	31.418	−82.326	47	Robertsdale loamy sand	Waycross 4 NE	26.0	18.9	11.8	1,271
244202	GA	Pierce	31.417	−82.325	47	Robertsdale loamy sand	Waycross 4 NE	26.0	18.9	11.8	1,271
246301	GA	Colquitt	31.305	−83.798	114	Tifton loamy sand	Moultrie 2 ESE	25.3	19.3	13.3	1,264
246302	GA	Colquitt	31.306	−83.798	114	Tifton loamy sand	Moultrie 2 ESE	25.3	19.3	13.3	1,264
246201	AL	Clarke	31.686	−87.963	57	Bama fine sandy loam	Jackson	24.8	18.2	11.6	1,529
249905	AL	Conecuh	31.511	−86.847	105	Troup loamy sand	Evergreen	24.8	18.3	11.7	1,550
249904	AL	Conecuh	31.442	−87.116	110	Troup loamy sand	Evergreen	24.8	18.3	11.7	1,550
249912	LA	Beauregard	30.815	−93.477	52	Doucette loamy fine sand	Leesville	25.2	18.6	12.1	1,465
241103	LA	Beaureguard	30.692	−93.486	48	Malbis fine sandy loam	Leesville	25.2	18.6	12.1	1,465
249909	TX	Jasper	30.838	−93.957	84	Doucette–Boykin association	Sam Rayburn Dam	24.2	19.0	13.8	1,518
249910	TX	Hardin	30.514	−94.390	33	Otanya very fine sandy loam	Wildwood	26.3	19.4	13.0	1,456
249907	TX	Liberty	29.997	−94.477	15	Orcadia–Aris complex	Liberty	25.8	20.2	14.6	1,556
249911	TX	Chambers	29.926	−94.408	12	Morey–Levac complex	Port Arthur Airport	25.7	20.6	15.3	1,536
249908	TX	Jefferson	29.921	−94.407	11	Morey–Levac complex	Beaumont City	25.6	20.3	14.9	1,535
249903	FL	Nassau	30.749	−81.861	7	Meggett loamy fine sand	Folkston 9 SW	27.6	20.8	14.1	1,315
249906	FL	Alachua	29.764	−82.266	51	Pomona sand	Gainesville Reg. Airport	26.7	20.5	14.3	1,202
245801	FL	Marion	29.484	−82.002	23	Pomona sand	Ocala	28.7	21.8	15.0	1,290
245805	FL	Marion	29.478	−81.994	22	Electra sand	Ocala	28.7	21.8	15.0	1,290
246101	FL	Glades	26.859	−81.399	14	Immokalee sand	LaBelle	28.8	22.3	15.9	1,345

was again sampled through nonparametric bootstrapping with replacement yielding a total of 125 unique datasets (n = 182) to examine the error associated with the volume model (Equation 11). The relation and clustering of parameters for each model form were examined for extraneous estimates (Figure 6).

Each of the sampling datasets (125 datasets; n = 22,750) with the respective parameter estimates was then projected for each plot (n = 22,750) from 1 to 14 years (n = 3,549,000) to evaluate the variance of each response variable (H, B, and V). SI was calculated for all plots within the bootstrapping analysis and grouped into SI classes as previously described. Current and mean annual increments were derived from the volume yield curve. The variance of the yield and rotation age was addressed by plotting histrograms for each MAI and respective rotation age by SI class.

Results and Discussion

Descriptive Statistics

The summary statistics for each age class for all sample plots (n = 182) are shown in Table 3. The trees per hectare (TPH) trend is due to increasing initial planting densities over time and not an indication of mortality. Although some age classes contain only one permanent sample plot, all modeling included all sample plots.

SI, Basal Area, and Yield Equations

The parameter estimates and their corresponding standard error terms are presented for each model form in Table 4. The overall model performance was evaluated based on the R^2, RMSE, BIC, and MBE as reported in Table 4. The Bailey–Clutter growth model (Equation 6) was found to fit the data best when compared to the other three dominant height growth equations as well as Equation 9, which included the relative spacing term (RS) for basal area growth estimation.

Although site quality was highly variable across all plots, the Bailey–Clutter model (Equation 6) was most effective at fitting the data to produce an SI curve for the height–age paired plot data for *E. benthamii*. The R^2 was 0.6786; however, given the wide range of data variation, we deemed this fit to be sufficient. Although this coefficient of determination appears low, Scolforo et al. (2013)

Table 3. Mean and standard deviation (in parentheses) of plot attributes (TPH, QMD, *B*, *H*, *V*, and DW) for each age class (year).

Age class (year)	Plots	TPH	QMD (cm)	B (m² ha⁻¹)	H (m)	V (m³ ha⁻¹)	DW (Mg ha⁻¹)
1	1	2,292	5.1	4.7	7.4	16.7	9.3
2	65	1,336 (288)	6.5 (1.5)	4.6 (1.9)	7.6 (1.3)	16.0 (8.1)	8.8 (4.5)
3	55	1,348 (210)	9.4 (1.6)	9.4 (2.8)	10.8 (1.7)	44.0 (19.6)	25.1 (11.7)
4	47	1,303 (239)	10.9 (1.7)	12.0 (2.9)	12.5 (1.7)	62.7 (19.3)	36.3 (11.6)
5	10	1,003 (150)	13.9 (3.0)	15.7 (6.6)	12.6 (1.3)	80.0 (33.4)	45.3 (19.0)
6	1	849	12.4	10.3	12.8	50.3	28.5
7	1	637	18.4	17.0	20.4	123.9	74.0
8	1	923	17.0	20.8	19.2	152.3	91.3
13	1	732	20.6	24.4	21.1	191.3	115.2

Note: B, basal area (m² ha⁻¹); *DW*, dry-weight biomass (Mg ha⁻¹); *H*, mean dominant height (m); QMD, quadratic mean diameter (cm); TPH, trees per hectare; *V*, volume (m³ ha⁻¹).

Table 4. Parameter estimates and standard errors, R^2, RMSE (in units respective to each model), BIC, and MBE for each model form.

Equation	Estimated coefficients				R^2	RMSE	BIC	MBE
Equation 3 (Schumacher)	β_0 = 3.04005 SE = 0.03592	β_1 = –2.02976 SE = 0.10990			0.6717035	1.63144	710.2701	0.00361
Equation 4 (Chapman–Richards)	β_2 = 22.72625 SE = 3.06457	β_3 = 0.17225 SE = 0.06211	β_4 = 0.86507 SE = 0.12415		0.6740393	1.625626	714.1746	–0.00386
Equation 5 (Logistic)	β_5 = 19.75912 SE = 1.40140	β_6 = 3.69411 SE = 0.35202	β_7 = –0.45731 SE = 0.05246		0.6557824	1.670531	724.0931	–0.00870
Equation 6 (Bailey–Clutter)	β_8 = 34.6928 SE = 12.4634	β_9 = –2.1999 SE = 0.2563	β_{10} = 0.5522 SE = 0.1784		0.6785687	1.614292	711.6279	–0.00166
Equation 7 (G—SinvA)	β_{11} = 3.50228 SE = 0.06484	β_{12} = –10.83769 SE = 0.53947	β_{13} = 0.44012 SE = 0.03412		0.8125518	1.301898	52.288858	1.03607
Equation 8 (G—Hdom:TPH)	β_{14} = –3.60258 SE = 0.69733	β_{15} = –1.57189 SE = 0.29198	β_{16} = 1.42314 SE = 0.11653	β_{17} = 0.40785 SE = 0.08703	0.8173138	1.297515	52.80923	1.03591
Equation 9 (G—Hdom:RS)	β_{18} = 0.8434 SE = 0.4880	β_{19} = –1.7007 SE = 0.2952	β_{20} = 0.9258 SE = 0.1560	β_{21} = –1.1496 SE = 0.2344	0.8192168	1.295751	50.90339	1.03484
Equation 11 (volume)	β_{22} = –0.40386 SE = 0.06048	β_{23} = 1.04695 SE = 0.01828	β_{24} = 0.76054 SE = 0.03917		0.9927752	1.073773	–424.5810	1.00247
Equation 11 (biomass)	β_{22} = –1.21050 SE = 0.07047	β_{23} = 1.04256 SE = 0.02130	β_{24} = 0.86525 SE = 0.04565		0.9907748	1.086475	–368.9233	1.00333

Note: BIC, Bayesian information criteria; MBE, mean bias error; R^2, coefficient of determination; RMSE, root mean square error; SE, standard error.

modeled *Eucalyptus* in Brazil with a coefficient of determination of 0.679 without the use of climate variables for clonal plantations showing the potential heterogeneous nature of *Eucalyptus* plantations across a given region. The lower R^2 value presented in this paper in comparison with Scolforo et al. (2013) is likely due to increased geographic range and the difference between *E. benthamii* germinated from seed compared to the single clone produced from vegetative propagation.

Equation 9 was also effective at fitting the data to predict stand basal area (m² ha⁻¹), and the R^2 was 0.8192, indicating the model was able to effectively explain the variation in basal area. Finally, Equation 11 was fitted to both yield metrics and was extremely robust for both yield metrics, stand-level volume and DW biomass, with R^2 terms of 0.9928 and 0.9908 respectively. These R^2 values are in agreement with those presented by Scolforo et al. (2018a).

Residual plots for each fitted equation are presented in Figure 3 showing the randomness of residuals distribution, indicating relative homogeneity in the variance and unbiased prediction equations. Although the observations at older stand ages have relatively low residual variance, it is important to state that these observations beyond year 6 have a significant influence on the model predictions.

Actual Productivity of *E. benthamii* in SE US

SI (S) for *E. benthamii* in the SE US ranged from 12.1 to 20.9 m with a mean of 17.3 m at a base age of 7 years (Figure 4a). The following SI model resulted in a family of polymorphic sigmoidal curves based on the assumption that the projection from Equation 6 (resulting in Equation 13) is polymorphic with a simple asymptote:

$$S = \beta_8 \left(\frac{H}{\beta_8}\right)^{\left(\frac{A_1}{A_b}\right)^{\beta_{10}}} \tag{12}$$

where A_1 is age in years when the dominant height was measured, A_b is the base age in years, and all other terms were previously defined. Plots were grouped using the following range of SI values to illustrate the differences in height across sites: SI-13 (11–14 m), SI-16 (14–18 m), and SI-19 (18–21 m). The 182 permanent sample plots are well distributed across all age classes at each SI class: 20 plots were identified as SI-19 class, 147 were identified as SI-16 class, and 15 were identified as SI-13 class (Table 5). Although Table 5 shows the limited range of SI in the data set because of the majority of the plots in SI-16 class, there is a reasonable distribution of plots in all age classes within each SI class.

Predicting basal area (m² ha⁻¹) as a function of age, dominant height, and *RS* (Equation 9) produced sensible estimates for basal area (Figure 4b). At age 7 years, SI-19 class had a mean basal area of 24.3 m² ha⁻¹. The basal area for SI-16 class was reduced by approximately 12.3 percent compared to SI-19 class, resulting in a mean of 21.3 m² ha⁻¹, and the mean basal area for SI-13 class was 16.4 m² ha⁻¹ at age 7 years. The basal area model resulted in a family of polymorphic sigmoidal curves. As expected, higher site qualities (i.e., SI-19 class) reached larger basal area values quicker than lower site qualities (i.e., SI-13 class).

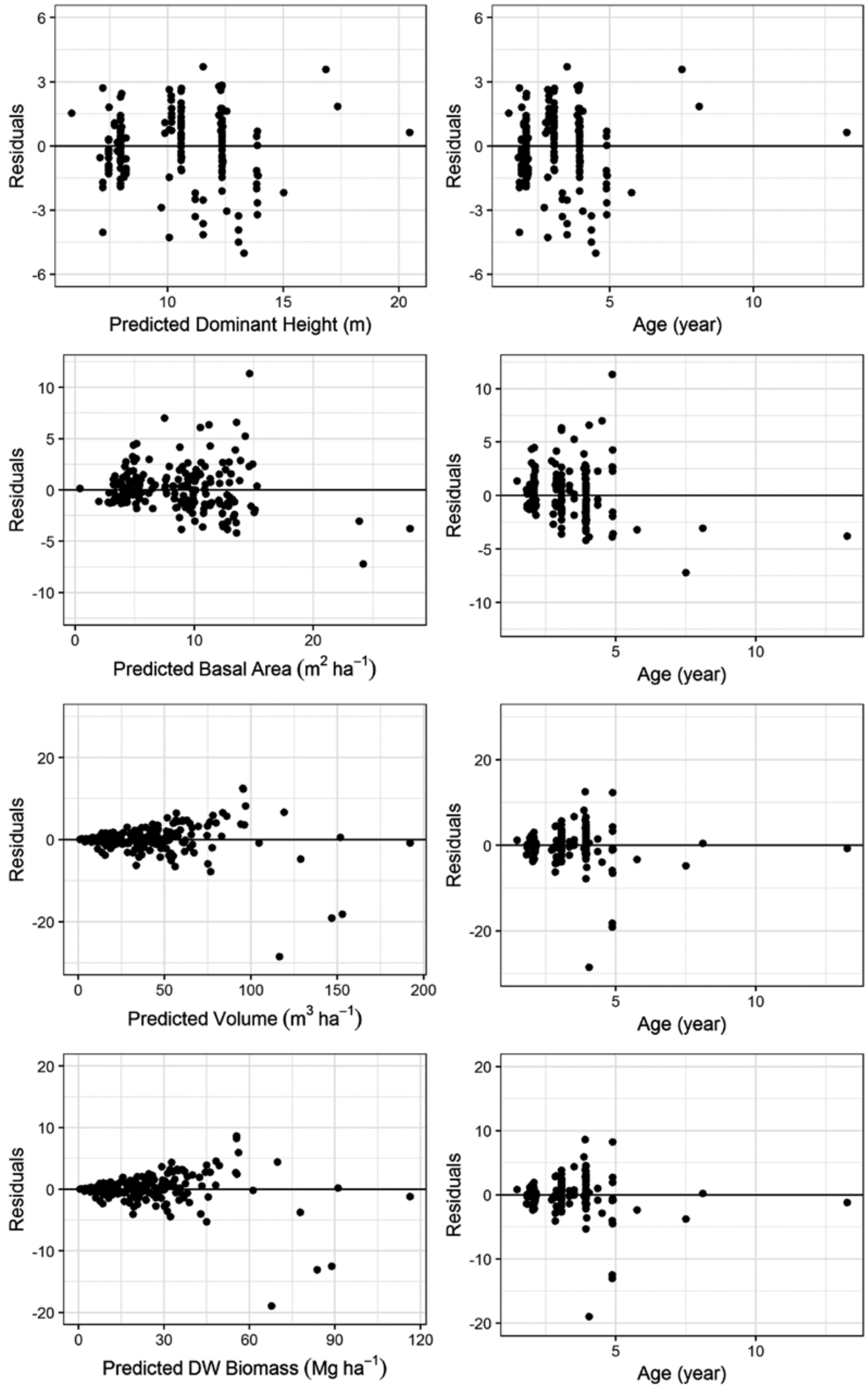

Figure 3. Residual plots by predicted value (left) and age (right) for each best fitting model (Equation 6—dominant height, Equation 9—basal area, and Equation 11—volume and biomass).

The actual productivity of *E. benthamii* in the SE US was predicted to determine yields at rotation age and evaluate growth. H (m) and B (m^2 ha^{-1}) at ages 1 through 15 years were predicted for each permanent sample plot using Equations 6 and 10, respectively (Figure 4c and d). Although the dataset used in the modeling exercise are limited to age 13 years, projections were made to year 15 to assure that rotation age and mean annual increment was obtained for all plots in the event that a specific plot had an estimated rotation age beyond 13 years. Equation 13 shows the transformation of Equation 12 to solve for a dominant height at a given age based on the SI, base age, and current age where all other terms were previously defined.

$$H = \beta_8 \left(\frac{S}{\beta_8} \right)^{\left(\left(\frac{A}{A_b} \right)^{-\beta_{10}} \right)} \quad (13)$$

For stand-level volume and DW biomass at age 7 years (Figure 4), the total yield was reduced by approximately 21 percent from SI-19 class to SI-16 class, 36 percent from SI-16 class to SI-13 class, and 49 percent from SI-19 class to SI-13 class. Stand-level volume ranged

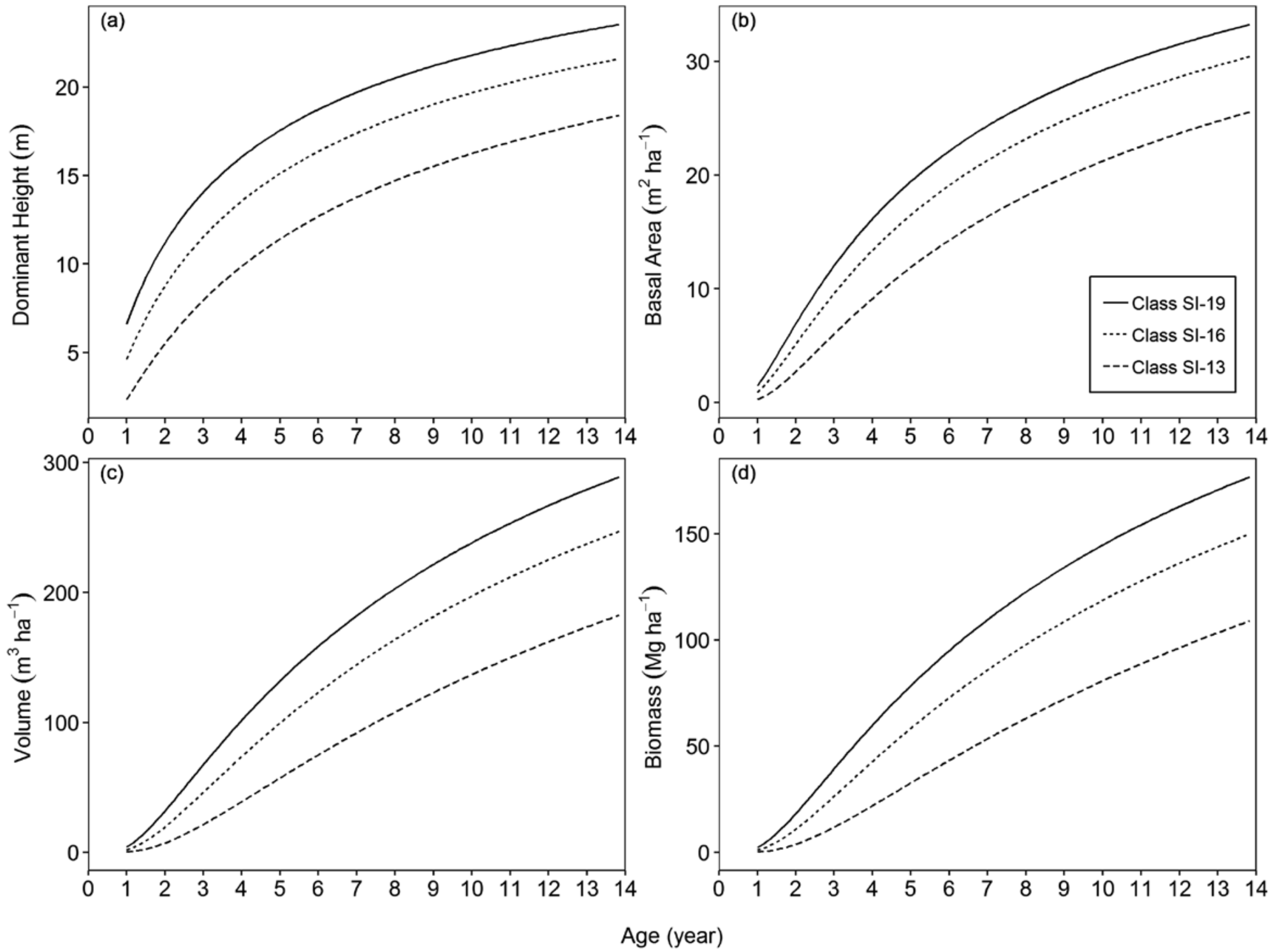

Figure 4. Mean predicted values for (a) dominant height (meters), (b) basal area (m² ha⁻¹), (c) stand-level volume (m³ ha⁻¹), and (d) dry weight biomass (Mg ha⁻¹) over time for *E. benthamii* in the southeastern United States. Mean dominant heights were predicted from Equation 6. The predicted mean basal area for each site index class was estimated from the model parameters of Equation 9. Predicted mean stand-level volume (m³ ha⁻¹) and dry weight biomass (Mg ha⁻¹) were estimated from the model parameters of Equation 11 for each yield type.

Table 5. Distribution of sample plots by site index and age classes.

SI class	Age class	*N*	Percentage
13	1	0	0
	2	1	7
	3	7	47
	4	5	33
	5	2	13
	>6	0	0
Total		15	100
16	1	0	0
	2	60	41
	3	39	27
	4	38	26
	5	8	5
	>6	2	2
Total		147	100
19	1	1	5
	2	4	20
	3	9	45
	4	4	20
	5	0	0
	>6	2	10
Total		20	100

from approximately 92.0 m³ ha⁻¹ for SI-13 class to 182.2 m³ ha⁻¹ for SI-19 class at age 7, whereas DW biomass ranged from approximately 53.4 Mg ha⁻¹ for SI-13 class to 109.6 Mg ha⁻¹ for SI-19 class at age 7.

MAI reported by Gonzalez et al. (2011) estimated yields for *E. benthamii* of 12.3 to 22.4 Mg ha⁻¹ year⁻¹ with rotation ages ranging from 7 to 8 years for the Lower Gulf Coast Region of the US. Potentially because the growth and yield model derived in this research encompassed a much larger region, results were lower at the maximum end with a greater overall range than those of Gonzalez et al. (2011). Our model estimated MAI ranging from approximately 8.1 to 15.8 Mg ha⁻¹ year⁻¹ DW and mean rotation ages ranging from approximately 10.8 to 6.3 years (Figure 5).

Eucalyptus production in other regions of the world ranges from an MAI as high as 62 m³ ha⁻¹ year⁻¹ for *E. grandis* × *urophylla* in tropical Brazil, 18–30 m³ ha⁻¹ year⁻¹ for *E. nitens* and *E. globulus* in Chile, and 20–25 m³ ha⁻¹ year⁻¹ for *E. nitens* in New Zealand (Tibbits et al. 1997, Stape et al. 2006). This model also indicates that *E. benthamii* in the SE US on above-average (SI-19 class) sites is producing as much volume as *E. nitens* and *E. globulus* in Chile, and *E. nitens* in New Zealand.

Eucalyptus species perform well in exotic environments when matched with an appropriate climate (Stape et al. 2010, Albaugh et al. 2013, Scolforo et al. 2018b). The SE US shows potential to support *E. benthamii*, with areas realizing MAIs ranging from approximately 13.7 (SI-13 class; rotation age 10.3 year) to 26.4 (SI-19 class; rotation age 6.1 year) m³ ha⁻¹ year⁻¹ depending on the site quality (Figure 5). In comparison, southern pines, predominantly

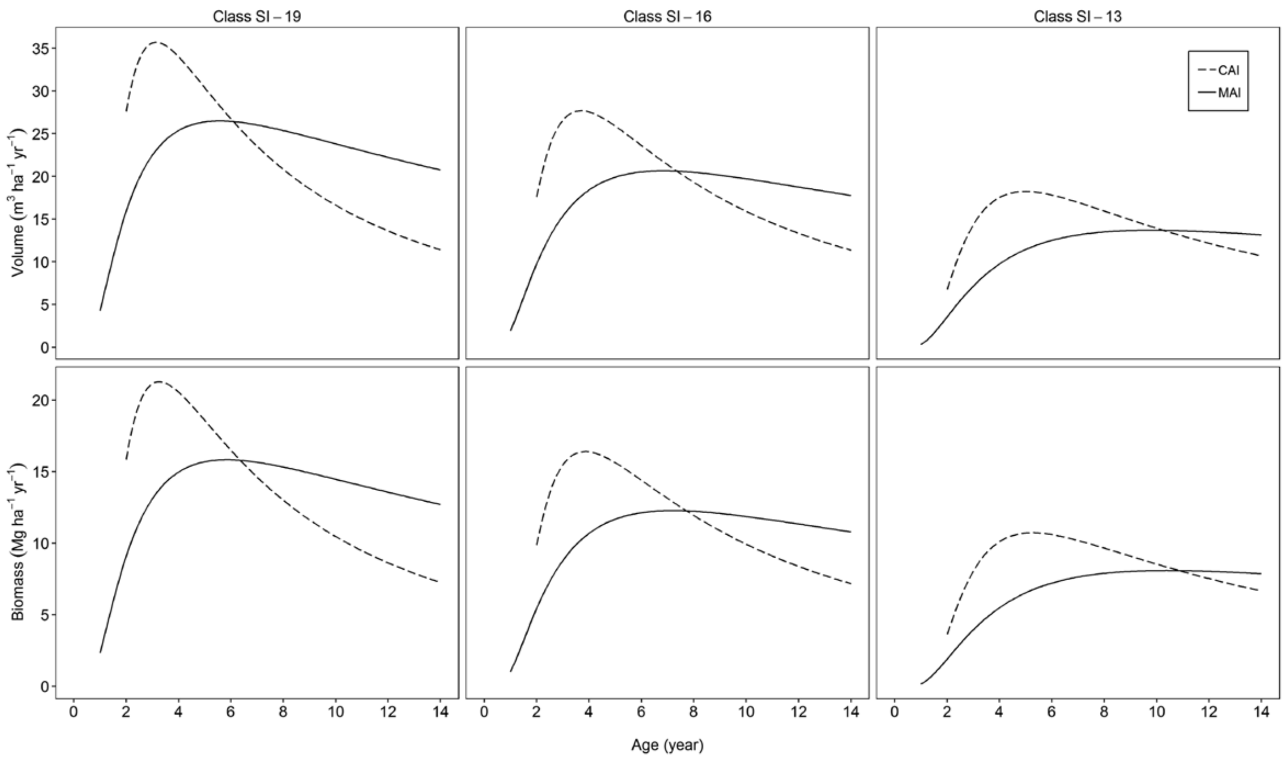

Figure 5. Mean for current (CAI; dotted line) and mean (MAI; solid line) annual increments for volume (m^3 ha^{-1} year^{-1}; upper panels) and biomass (Mg ha^{-1} year^{-1}; lower panels) by site index class for *E. benthamii* in the southeastern United States.

loblolly pine (*Pinus taeda* L.) and slash pine (*P. elliottii* Englem.), but including shortleaf (*P. echinata* Mill.), longleaf (*P. palustris* Mill.), pond (*P. serotina* Michx.), sand (*P. clausa* Chapm.), and Virginia (*P. virginiana* Mill.) pines, typically produce 7–15 m^3 ha^{-1} year^{-1} and as much as nearly 30 m^3 ha^{-1} year^{-1} over a 25–30-year rotation under plantation management in the same region of the United States (Allen et al. 1990, Fox et al. 2007).

E. benthamii in the SE US on average sites (SI-16 class) produces 20.6 m^3 ha^{-1} year^{-1} with an average rotation age of 7.3 years. Stanturf et al. 2018 calibrated 3-PG processed-based model for *E. benthamii* and *E. grandis* in the SE US where the same parameter inputs were used for both species with the exception of the frost modifier, specific leaf area, and wood density. Their results showed that mean production based on a 5-year rotation was 21.9 m^3 ha^{-1} year^{-1} with a range of 3.3–76 m^3 ha^{-1} year^{-1} (Stanturf et al. 2018). Although our results are complementary to those of Stanturf et al. 2018, it should be noted that the rotation age based on the processed-based model (5 years) should be considered with caution, as it does not consider longer rotations on sites with lower productivity. Even with limited data used in the construction of this model, forest managers and scientists will be able to use these models to access more accurately the production, value, and sustainability of *E. benthamii* in the SE US.

Model Stability, Error Propagation, and Variance of the Results

The development of an independent set of prediction equations to build a recursive G & Y model, the fact that most of the plots in this study are concentrated at younger ages, and the majority of the plots falling into one SI class have an impact with regard to the uncertainty related to the system of equations used in the development of the overall model. Nonparametric bootstrapping with replacement was performed for each model form beginning with the Bailey–Clutter dominant height model and was repeated throughout the system of equations, exponentially increasing the number of simulated datasets, until reaching the final volume model to assess the stability of the models. The variation of the parameter estimates associated with each sample dataset is presented in Figure 6. The figure shows the clustering and range of parameter estimates associated with each model form. Although linearity is observed among some parameters in the system of equations, clustering is observed for the majority of the parameters with good precision in the volume model.

Figure 7 shows the projected dominant height, basal area, and volume of all sample plots in the uncertainty analysis. Using the dominant height projections to determine SI, plots were grouped by SI class as previously described. CAI and MAI were then calculated for each plot, and the confidence intervals related to MAI and rotation age are presented in Figure 8.

Uncertainty analyses revealed the variation associated with the means for MAI and rotation age distributions for stand-level volume (Figure 8). The uncertainty analysis shows large variations among plots with productivity ranging from 8.5 m^3 ha^{-1} year^{-1} at SI-13 to 29.9 m^3 ha^{-1} year^{-1} at SI-19. Rotation ages consistently reflected the variation with a range of 4.3–11.9 years. Additionally, at SI-19 in Figure 8, some plots were projected to have MAIs as high as 40 to nearly 50 m^3 ha^{-1} year^{-1}. Although these projections are extreme, they are considerably lower than and within the range of the potential productivity reported by Stanturf et al. 2018. The uncertainty analysis showed that the models presented described the growth of *Eucalyptus benthamii* in the SE US while accounting for the large variability associated with the introduction of a new species into an exotic environment. The confidence intervals associated with the uncertainty

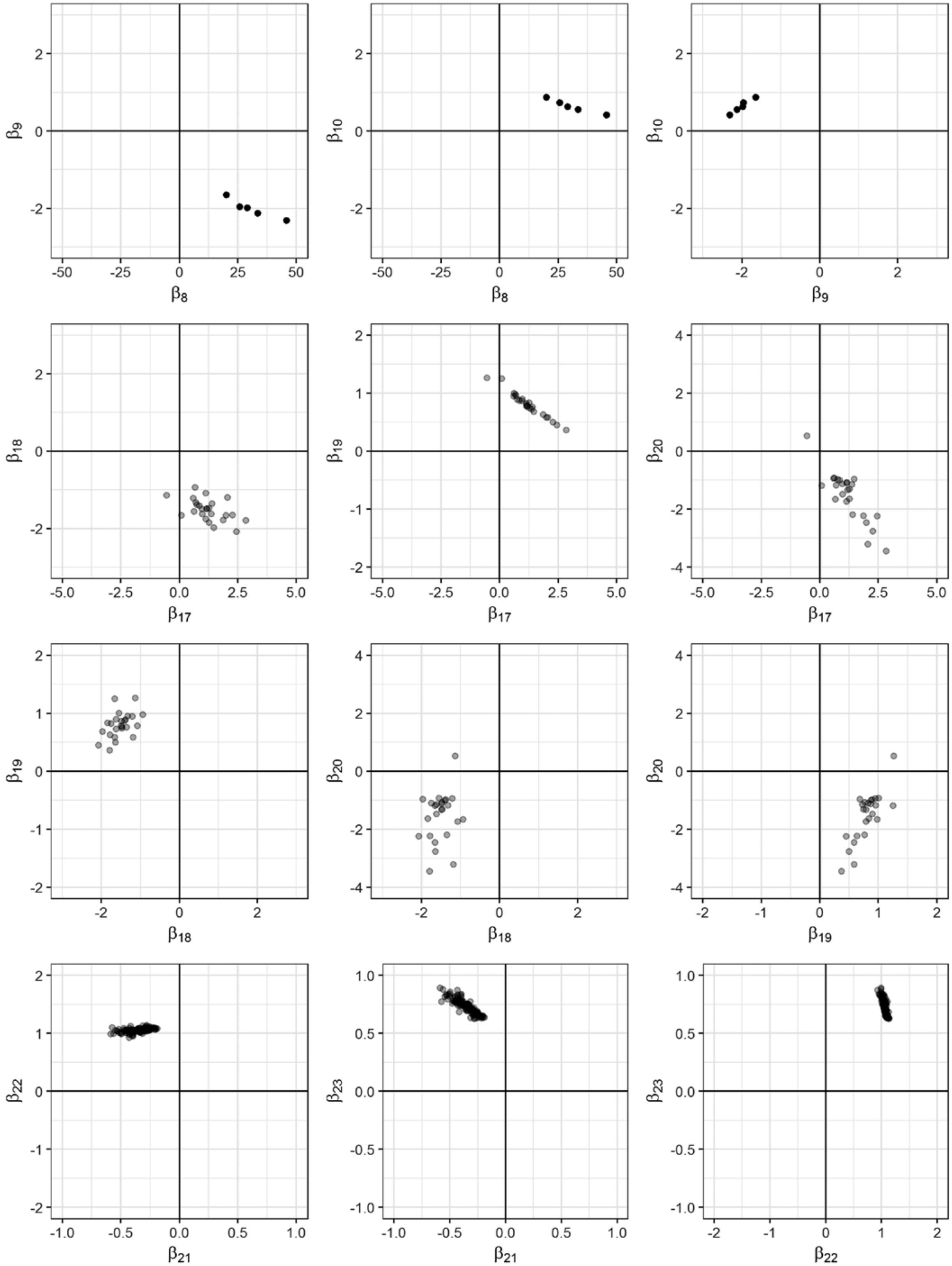

Figure 6. Distribution of parameter estimates for each simulated dataset from the nonparametric bootstrapping. The top three figures are relations of the parameters in the dominant height model (Equation 6), the middle six figures are the relations of the parameters of the basal area model (Equation 9), and the bottom three figures are the relations of the parameters in the volume model (Equation 11).

analysis show that the variation associated with mean MAI and rotation age for each SI class can be considered substantial, and this model should be applied to future *E. benthamii* stands with caution.

It is important to state that this is the first study that has furnished estimates with regard to *E. benthamii* productivity in SE US, and that most of the available data used for building the G & Y model are less than the rotation age range reached as the conclusion. Hence, the key conclusion with regard to MAI of volume should be treated carefully, since future data collection must be incorporated in the G & Y model. Furthermore, these models will

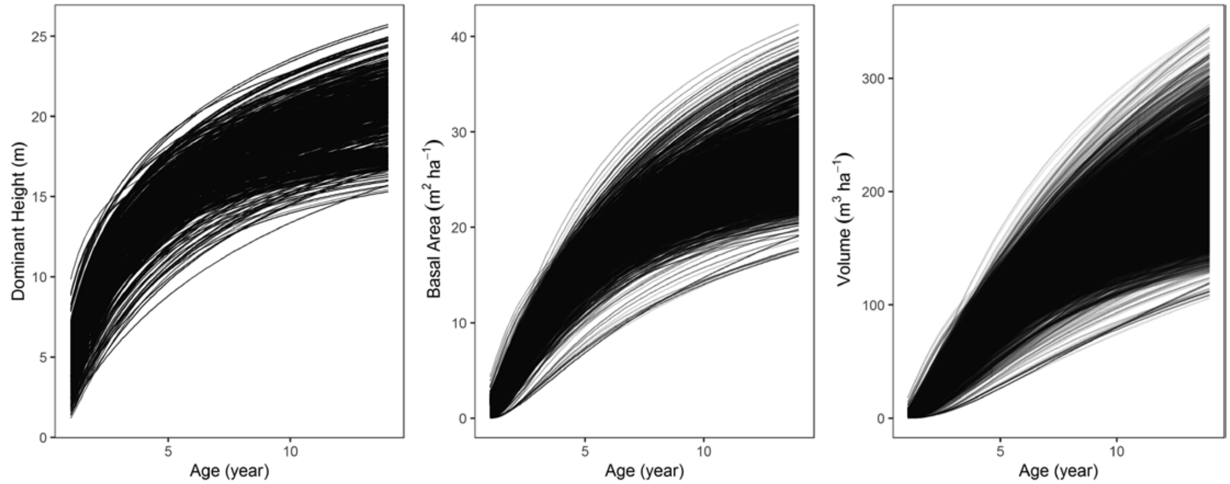

Figure 7. Projected dominant height (m), basal area (m² ha⁻¹), and volume (m³ ha⁻¹) for each plot (*n* = 22,750) in the datasets generated in the nonparametric bootstrapping analysis.

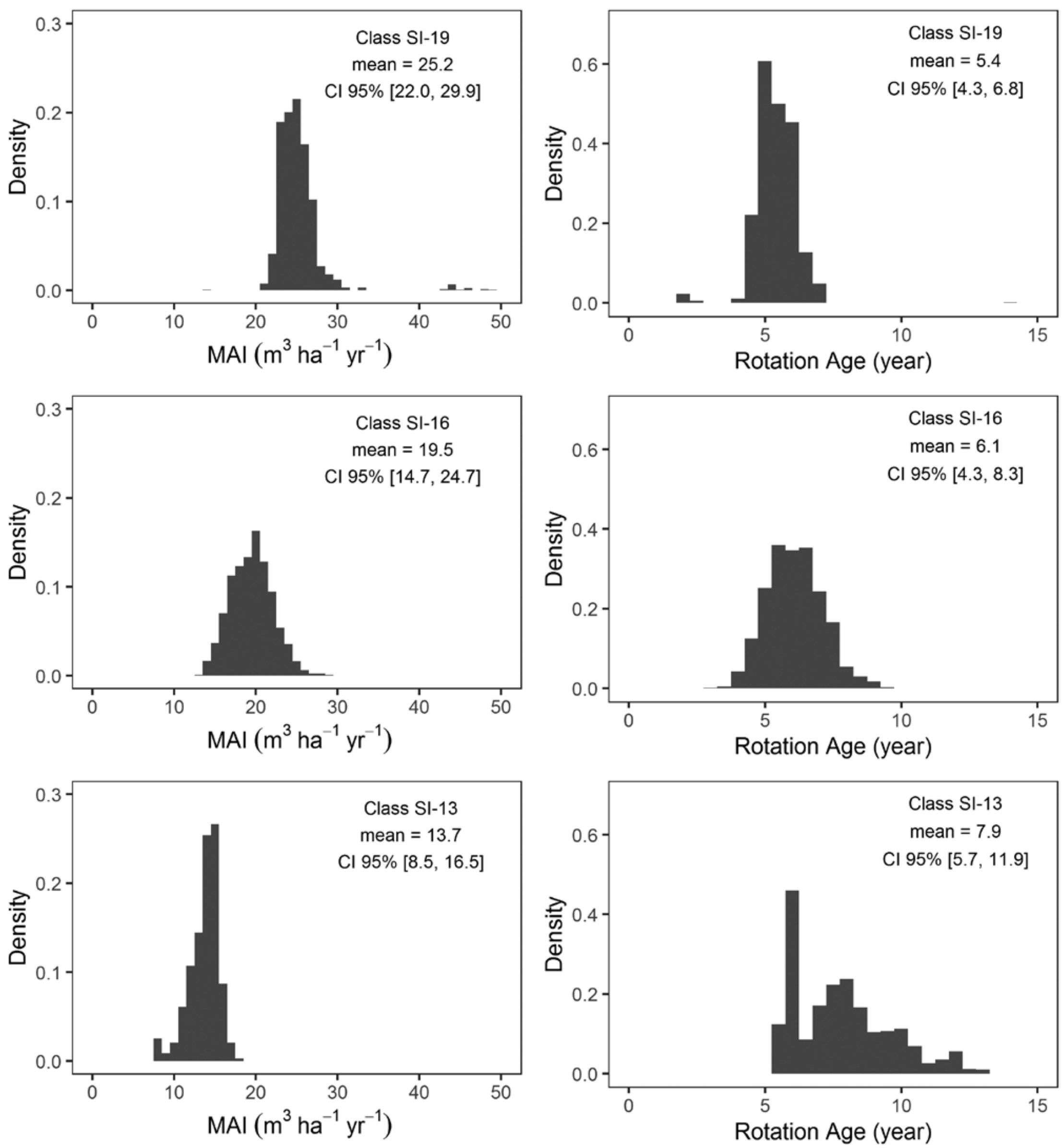

Figure 8. Histogram, mean, and 95 percent confidence intervals for mean annual increment (m³ ha⁻¹ year⁻¹) and rotation age (year) for all plots in the nonparametric bootstrapping derived from the projected volume of all plots.

need to be revisited, as the potential productivity for *E. benthamii* is much greater than what has been observed in these initial plantings and trials with improvements in genetic material through breeding and vegetative propagation and silvicultural improvements.

Conclusions

E. benthamii growth and yield models show a wide range of productivity across varying edaphic and climatic conditions. SI at a base age of 7 years ranged greatly from approximately 12.1 to 20.9 m, depending on the variability in site quality. MAI can range from 13.7 to 26.4 m^3 ha^{-1} $year^{-1}$ at rotation ages ranging from 10.3 (low site productivity) to 6.1 (high site productivity) years, respectively.

The empirical data of *E. benthamii* trials in the SE US show that the actual productivity is promising. Although the potential productivity of *E. benthamii* in the SE US is defined by factors such as genotype, edaphic, and climatic conditions, silvicultural practices may eliminate reducing factors (i.e., pests, diseases, and competing vegetation) and alleviate limiting factors (i.e., nutrition), which will ultimately narrow the gap between the actual and potential productivity of *E. benthamii* in the SE US.

Literature Cited

Albaugh, J.M., P.J. Dye, and J.S. King. 2013. Eucalyptus and water use in South Africa. *Int. J For. Res.*. 2013: Article ID 852540, 11.

Allen, H.L., P.M. Dougherty, and R.G. Campbell. 1990. Manipulation of water and nutrients—practice and opportunity in Southern U.S. pine forests. *For. Ecol. Manag*. 30: 437–453.

Allen, H.L., T.R. Fox, and R.G. Campbell. 2005. What is ahead for intensive pine plantation silviculture in the South? *South. J. Appl. For.* 292(2): 62–69.

Arguez, A., I. Durre, S. Applequist, R.S. Vose, M.F. Squires, X. Yin, R.R. Heim, Jr., and T.W. Owen. 2012. NOAA's 1981–2010 U.S. climate normals: An overview. *Bull. American Meteorol. Soc.* 93: 1687–1697.

Burkhart, H.E., and M Tomé. 2012. *Modeling forest trees and stands*. Springer Science Business Media, Dordrecht.

Curtis, R.O. 1967. Height–diameter, and height–diameter–age equations for second growth Douglas-fir. *For. Sci*. 13: 365–375.

Fox, T.R., E.J. Jokela, and H.L. Allen. 2007. The development of pine plantation silviculture in the Southern United States. *J. For*. 105(7): 337–347.

Goerndt, M.E., and C. Mize. 2008. Short-rotation woody biomass as a crop on marginal lands in Iowa. *North. J. Appl. For*. 25: 82–86.

Gonzalez, R., T. Treasure, J. Wright, D. Saloni, R. Phillips, R. Abt, and H. Jamaal. 2011. Exploring the potential of *Eucalyptus* for energy production in the Southern United States financial analysis of delivered biomass. *Part I. Biomass and Bioenergy*. 35: 755–766.

Hall, K.B. 2015. *Modeling the actual productivity of* Eucalyptus benthamii *in the Southeastern United States.* Thesis, NCSU, 161 p.

Headlee, W.L., R.S. Zalesny, D.M. Donner, and R.B. Hall. 2013. Using a process-based model 3-PG to predict and map hybrid poplar biomass productivity in Minnesota and Wisconsin, USA. *Bioenerg. Res.*. 6: 196–210.

Kellison, R.C., R. Lea, and P. Marsh. 2013. Introduction of *Eucalyptus* spp. into the United States with special emphasis on the Southern United States. *Intern. J. For. Res*. 2013: 9.

Mcroberts, R.E., and J.A. Westfall. 2014. Effects of uncertainty in model predictions of individual tree volume on large area volume estimates. *For. Sci*. 60(1): 34–42.

Mujiu, L., R. Arnold, L. Bohai, and Y. Minsheng. 2003. Selection of cold-tolerant eucalypts for Hunan province. P. 107–117 in *Eucalyptus* in Asia: Proceedings of a international conference held in Zhanjiang, J.W. Turnbull (ed.). April 7–11, Guangdong, People's Republic of China. ACIAR. (ACIAR. Proceedings, 111).

Netzer, D.A., D. Tolsted, M.E. Ostry, J.G. Isebrands, D.E. Riemenschneider and K.T. Ward. 2002. Growth, yield, and disease resistance of 7- and 12-year-old poplar clones in the north central United States. USDA Forest Service Gen. Tech. Rep. NC-229, North Central Research Station, St. Paul, MN. 21 p.

Perlack, R.D., L.L. Wright, A.F. Turhollow, R.L. Graham, B.J. Stokes, and D.C. Erbach. 2005. *Biomass as feedstock for a bioenergy and bioproducts industry: The technical feasibility of a billion-ton annual supply.* US Department of Energy, Oak Ridge National Laboratory, Oak Ridge, TN. 59 p.

Pienaar, L.V., and B.D. Shiver. 1986. Basal area prediction and projection equations for pine plantations. *For. Sci*. 32(3): 626–633.

Rockwood, D.L. 2012. History and status of eucalyptus improvement in Florida. *Intern J For. Res.* 2012: Article ID 607879. 10.

Rockwood, D.L., A.W. Rudie, S.A. Ralph, J.Y. Zhu, and J.E. Winandy. 2008. Energy product options for *Eucalyptus* species grown as short rotation woody crops. *Int. J. Sci.* 9: 1361–1378.

R Core Development Team. 2015. *R: A language and environment for statistical computing.* R Foundation for Statistical Computing, Vienna. Available online at http://www.R-project.org; last accessed March 1, 2016.

Schultz, R.P. 1997. *Loblolly pine. The ecology and culture of loblolly pine (Pinus taeda L.). Agricultural handbook 713*. US Forest Service, Washington, DC.

Schumacher, F.X. 1939. A new growth curve and its application in timber—yield. *J. For*. 37: 817–820.

Scolforo, J.R.S., R. Maestri, A.C.F. Filho, J.M. De Mello, A.D. De Oliveira, and A.L. De Assis. 2013. Dominant height model for site classification of *Eucalyptus grandis* incorporating climate variables. *Int. J For. Res.* 2013: Article ID. 139236. 7.

Scolforo, H.F., F.C. Neto, J.R.S. Scolforo, H. Burkhart, J.P. Mctague, M.R. Raimundo, R.A. Loos, S. Fonseca, and R.C. Sartorio. 2016. Modeling dominant height growth of eucalyptus plantations with parameters conditioned to climatic variations. *For. Ecol. Manag.* 380: 182–195.

Scolforo, H.F., J.R.S. Scolforo, J.L. Stape, J.P. Mctague, H. Burkhart, J. Mccarter, F. De Castro Neto, R.A. Loos, and R.C. Sartorio. 2017. Incorporating rainfall data to better plan eucalyptus clones deployment in eastern Brazil. *For. Ecol. Manag.* 391: 145–153.

Scolforo, H.F., J.P. McTague, H. Burkhart, J. Roise, O. Campoe, and J.L. Stape. 2018a. Eucalyptus growth and yield system: Linking individual-tree and stand-level growth models in clonal Eucalypt plantations in Brazil. *For. Ecol. Manag.* 432(15): 1–16.

Scolforo, H.F., J.P. McTague, H. Burkhart, J. Roise, O. Campoe, and J.L. Stape. 2018b. Yield pattern of Eucalypt clones across tropical Brazil: An approach to clonal grouping. *For. Ecol. Manag.* 432(15): 30–39.

Simmons, B.A., D. Loque, and H.W. Blanch. 2008. Next-generation biomass feedstocks for biofuel production. *Genome Biol.* 9: 242.

Soil Survey Staff, Natural Resources Conservation Service, United States Department of Agriculture. Web Soil Survey. Available online at https://websoilsurvey.sc.egov.usda.gov/; last accessed February 21, 2019.

Stanturf, J.A., J.P. T.m. Young, and X. Huang. 2018. Productivity and profitability potential for non-native *Eucalyptus* plantings in the southern USA. *For. Policy Econ*. 97: 210–222.

Stape, J.L., D. Binkley, W.S. Jacob, and E.N Takahashi. 2006. A twin-plot approach to determine nutrient limitation and potential productivity in *Eucalyptus* plantations at landscape scales in Brazil. *For. Ecol. Manag.* 223: 358–362.

Stape, J.L., D. Binkley, M.G. Ryan, S. Fonseca, R.A. Loos, E.N. Takahashi, C.R. Silva, et al. 2010. The Brazil *Eucalyptus* potential productivity project influence of water, nutrients and stand uniformity on wood production. *For. Ecol. Manag.* 259: 1684–1694.

Tibbits, W.N., D.B. Boomsma, and S. Jarvis. 1997. Distributions, genetics and improvement programs for *Eucalyptus globulus* and *Eucalyptus nitens* around the world. P. 81–98 in *Proceedings of the 24th Biennial, Southern Forest Tree Improvement Conference*, White, T., D. Huber, and G. Powell (eds.) June 9–12, 1997. University of Florida, Orlando, FL.

Wang, Z., and D.W. Macfarlane. 2012. Evaluating the biomass production of coppiced willow and poplar clones in Michigan, USA, over multiple rotations and different growing conditions. *Biomass Bioenergy* 46: 380–388.

Zalesny, R.S. Jr., M.W. Cunningham, R.B. Hall, J. Mirck, D.L. Rockwood, R.A. Stanturf, and T.A. Folk. 2011. Woody biomass from short rotation energy crops. P. 27–63 in *Sustainable production of fuels, chemicals, and fibers from forest biomass*, Zhu, J., X. Zhang, and X. Pan (eds.). ACS Symposium Series; American Chemical Society, Washington, DC.

Zhao, D., M. Kane, and B.E. Borders. 2012. Crown ratio and relative spacing relationships for loblolly pine plantations. *Open J. For*. 2: 110–115.